Parallel Arrays of Josephson Junctions for Submillimeter Local Oscillators

Aleksandar Pance* and Michael J. Wengler

Department of Electrical Engineering
University of Rochester
Rochester, NY 14627

Abstract

In this paper we discuss the influence of the DC biasing circuit on operation of parallel biased quasioptical Josephson junction oscillator arrays. Because of nonuniform distribution of the DC biasing current along the length of the bias lines, there is a nonuniform distribution of magnetic flux in superconducting loops connecting every two junctions of the array. These DC self-field effects determine the states of the array. We present analysis and time-domain numerical simulations of these states for four biasing configurations. We find conditions for the in-phase states with maximum power output. We compare arrays with small and large inductances and determine the low inductance limit for nearly-in-phase array operation. We show how arrays can be steered in H-plane using the externally applied DC magnetic field.

Introduction

The Josephson junction is a natural choice for submillimeter local oscillator since it is a "voltage controlled oscillator" with typical voltage scales of mV and an oscillation frequency f_J = 483 GHz per mV of dc bias. The existence of Josephson radiation into the terahertz range has been demonstrated at Cornell [1]. A major disadvantage of the Josephson junction is its very low output power. With DC voltage bias of 1 mV at 483 GHz, a junction which could accept 100 μA will put out less than 100 nW of RF power. Therefore, practical local oscillators must use arrays of many junctions oscillating in phase. Submillimeter Josephson oscillator arrays with usable power levels have been made at Stony Brook [2] and NIST [3].

We have proposed to build a large 2-D active grid array of parallel biased Josephson junctions [4]. In our design, every junction drives a single antenna and the power from the whole array is quasioptically combined. By biasing all junctions in parallel, we assure that all of them

---

* 1991 Link Energy Foundation Fellow.

radiate at exactly the same frequency. For maximum radiated power, all junctions must also be in phase.

The DC biasing circuit of the 2-D quasioptical Josephson array plays a very important role in phase-locking of Josephson junctions. In a two-dimensional array the DC biasing current is supplied at the ends (Fig. 1). Because of that, the DC current is nonuniformly distributed along the length of the biasing line. This current induces the nonuniform DC magnetic flux in superconducting loops between every two neighboring junctions. Because of the superconducting quantum interference effects [5], these self-induced fluxes determine the phase differences between the neighboring junctions, and therefore the states of the array. These effects will be referred to as the DC self-field effects. It is clear that, depending on the particular bias circuit, the in-phase state can only be a special, rather than common state of the parallel 2-D Josephson junction array.

If the rows of the 2-D parallel Josephson array are biased independent from each other, the DC self-field effects are, to the first order, limited to each row, and the whole 2-D array can be looked at as a collection of 1-D parallel arrays. We will therefore investigate these DC self-field effects in linear parallel arrays.

N-junction linear parallel array

The most general biasing scheme for the linear parallel array is presented in Fig. 2. We use the RSJC model of the Josephson junction that consists of ideal Josephson junction, shunt resistance and parasitic capacitance (Fig. 2). The ideal Josephson junction is described by relationships between its current I, voltage V and phase difference ϕ of the superconducting quantum mechanical wave function between two sides of the junction

$$I = Ic \sin(\phi), \quad \frac{d\phi}{dt} = \frac{2e}{\hbar} V$$

where Ic is the junction critical current. Assuming that all junctions are identical, the circuit from Fig. 2 can be described with the following system of equations:

$$i_1(\tau) = \frac{1}{\lambda}(\phi_2(\tau)-\phi_1(\tau)) + \frac{\gamma_1}{2} - \frac{\gamma_R}{2} - \frac{2\pi}{\lambda}\varphi_{ex}$$

$$i_j(\tau) = \frac{1}{\lambda}(\phi_{j+1}(\tau)-2\,\phi_j(\tau)+\phi_{j-1}(\tau)) + \frac{\gamma_j}{2}, \qquad j = (2, N-1)$$

$$i_N(\tau) = -\frac{1}{\lambda}(\phi_N(\tau)-\phi_{N-1}(\tau)) + \frac{\gamma_N}{2} + \frac{\gamma_L}{2} + \frac{2\pi}{\lambda}\varphi_{ex} \qquad (1.a)$$

where ϕ_j is the superconducting wave function phase difference across the j^{th} junction, i_j is the total current through the j^{th} junction, γ_j, γ_L and γ_R are biasing currents and φ_{ex} is the normalized externally applied DC magnetic flux,

$$i_j(\tau) = \beta\ddot{\phi}(\tau) + \dot{\phi}(\tau) + \sin(\phi(\tau))$$

$$\gamma_j = i_{Uj} + i_{Dj},$$

$$\gamma_L = i_{L\,in} + i_{L\,out}, \quad \gamma_R = i_{R\,in} + i_{R\,out}$$

$$\varphi_{ex} = \frac{\Phi_{ex}}{\Phi_0} \qquad (1.b)$$

with capacitance and inductance parameters β and λ, respectively, given by

$$\beta = \frac{R^2 C}{L_j}, \quad \lambda = \frac{L}{L_j}, \quad L_j = \frac{\Phi_0}{2\pi I_c}, \quad \Phi_0 = \frac{h}{2e} \qquad (1.c)$$

where L_j is the zero-bias Josephson junction inductance and $\Phi_0 = 2.07 \times 10^{-15}$ Wb is the flux quantum. In equations (1.a-c), time is given in units of $\frac{L_j}{R}$, all currents in units of I_c and normalized junction voltages, that are just time derivatives of junction phases ϕ_j, in units of I_cR.

In the case of 2-junction array, the in-phase solution has been reported by Ben-Jakob et al [6]. Here we present solutions for several N-junction arrays with different biasing configurations: the LL ("left"-"left"), LR ("left"-"right"), UD ("up"-"down") and CB ("central bias") biased array (Fig. 3). Although the LL and LR bias are directly applicable to parallel biased two-dimensional arrays, the other two configurations are used in other array architectures, such as series-parallel combinations, etc.

In-phase states

The general solution of eq. (1) for the junction phases ϕ_j is

$$\begin{aligned} \phi_j(\tau) &= \omega\tau + f_j(\tau) + \phi_j(0) \\ \omega &= \left\langle \dot{\phi}_j(\tau) \right\rangle \\ f_j(\tau+T) = f_j(\tau), \quad T &= \frac{2\pi}{\omega}, \quad \left\langle \dot{f}_j(\tau) \right\rangle = 0 \end{aligned} \tag{2}$$

where "< >" denotes time average, ω is the normalized DC voltage across junctions, f_j's are some general, periodic functions with zero time-average and $\phi_j(0)$ are constants. For the in-phase solution, the following condition must hold for every two neighboring junctions

$$\phi_{j+1}(\tau) - \phi_j(\tau) = 2\pi m_j \tag{3}$$

where m_j must be an integer. Note that m_j represents the number of fluxons in the j^{th} loop.

Condition (3) is fulfilled if

$$\begin{aligned} f_j(\tau) &= f(\tau) \\ \phi_{j+1}(\tau) &= \phi_j(\tau + \tau_j) \\ \tau_j &= m_j T \end{aligned} \tag{4}$$

where τ_j is the time delay between the phases of the two neighboring junctions. Substituting (3) into the system (1.a) and equating all the currents i_j leads solutions

$$m_j = j\,a + \varphi_{ex} \qquad \text{(LL bias)} \tag{5.a}$$

$$m_j = (j - \frac{N}{2})\,a + \varphi_{ex} \qquad \text{(LR bias)} \tag{5.b}$$

$$m_j = \varphi_{ex} \qquad \text{(UD bias)} \tag{5.c}$$

$$m_j = ([\frac{N}{2}] - j)\,a + \varphi_{ex} \qquad \text{(CB bias)} \tag{5.d}$$

where "" in eq. 5.d denotes integer division, and parameter 'a' is given by

$$a = \frac{\lambda\, i_{DC}}{2\,\pi\, N} \tag{6}$$

where i_{DC} is the total DC biasing current. In order for m_j to be an integer, which is the precondition for the in-phase solution, it is necessary that both φ_{ex} and a be integers:

$$\varphi_{ex} = k_{\varphi}$$
$$a = \frac{\lambda\, i_{DC}}{2\,\pi\, N} = k \tag{7}$$

where k_{φ} and k are integers. The only exception is the LR array with odd number of junctions N, where "a" must be an even integer (2 k). The arrays will be in phase for all currents i_k that satisfy

$$i_k = k\,\frac{2\,\pi\, N}{\lambda} \tag{8}$$

Note that these in-phase states are achieved without external locking mechanisms.

Numerical simulations

System (1) is solved numerically using the 4th order Runge-Kutta method [7]. Figure 4 shows the I-V and dV/dI-I curves of the 4 junction LL biased array with λ=20 and β=0.5. According to eq. (8), the in-phase states appear for current bias i_k= 1.256 k (i_k'=0.314 k for bias current normalized to the number of junctions, N, as in the Figure 4). The in-phase states are visible as voltage maximums in the I-V curve and sharp and deep minimums in dV/dI-I curve, for k=4 to 7. Similar structure has been observed experimentally by Clarke et al [8].

Other states

The dV/dI-I curve of Figure 4 reveals considerable periodic structure between the in-phase states. Under certain conditions, that will be specified below, these "other" states, for current bias $i_{DC} \neq i_k$, correspond to the general solution of eq. (2) that satisfies the following:

$$f_{j+1}(\tau) - f_j(\tau) = \varepsilon_j(\tau)$$
$$\phi_{j+1}(\tau) \approx \phi_j(\tau + \tau_j)$$
$$\tau_j \approx \mu_j T \qquad \forall j \tag{9}$$

where $\varepsilon_j(\tau)$ is an error term and μ_j does not need to be an integer. Furthermore, μ_j is found from the same equations as m_j (5), except that a and φ_{ex} are no more restricted to integer numbers. In other words, all states of the parallel array are described with phases at neighboring junctions shifted in time by an amount determined by the DC biasing current and external magnetic field (eq. 5). It is convenient to define the relative normalized time shift θ_j between the waveforms of functions f_{j+1} and f_j

$$\theta_j = \tau_j \bmod T = \mu_j \bmod 1 \qquad (10)$$

where "mod" is the modulus function, so that $0 \le \theta_j \le 1$. It has been shown by perturbation analysis [6] that in the case of 2-junction array solution (9) holds in the neighborhood of the in-phase state ($i_{DC} = i_k + \Delta i_{DC}$) and it has been suggested that it will hold for any state between the in-phase states, for the case of weak coupling ($\lambda >> 1$).

Figure 5.a shows the circled part of the dV/dI-I curve of Fig. 4. Points labeled "1" and "4" correspond to the in-phase states with k=4 and k=5, respectively. The voltage waveforms on individual junctions for these two states are shown in Figures 6.a and 7.a, respectively. Point "2" of Fig. 5.a correspond to DC biasing current $i_{DC} = 5.65$, so eq. (5.a) gives $\mu_1=4.5$, $\mu_2=5$ and $\mu_3=5.5$ for the number of fluxons in each loop. From eq. (10) we find that relative time shifts should be $\theta_1=0.5$ between the voltages of the junctions 2 and 1, $\theta_2=0$ for junctions 3 and 2 and $\theta_3=0.5$ between junctions 4 and 3. Numerical simulations shown in Figure 6.b confirm this prediction.

Point "3" of Fig. 5.a correspond to $i_{DC} = 5.42$, and again from equations (5.a) and (10) we obtain $\theta_1=0.333$, $\theta_2=0.666$ and $\theta_3=0$. The voltage (and phase) at junction 2 is time shifted by third of a period from that of junction 1, voltage at junction 3 is shifted by two-thirds from that of junction 2, so that it is in phase with junction 1. Finally, junction 4 is in phase with junctions 1 and 3. This situation is shown in Figure 6.c. All other states can be determined in a similar fashion.

Radiated power

As a measure of how good an array performs as an oscillator for a particular bias, we calculate the available radiation power. We are interested in power array would radiate broadside in the far-field. We define m^{th} harmonic power on unit (1 Ω) resistance as

$$P^{(m)} = (\Sigma V_j^{(m)})^2$$

where $V_j^{(m)}$ is m^{th} harmonic voltage on j^{th} junction. This power is given in units of $(Ic\ R)^2$. We assume that the resistance R of the RSJC model (Fig. 2) includes both the radiation resistance and losses. The actual radiated power will at best be the power $P^{(m)}$ on resistance $\frac{R}{2}$.

Figure 5.b shows the normalized first harmonic power radiated in the broadside direction for different states of the array. The maximum power is obtained only in the in-phase states (points "1" and "4"). Significant amount of power is also obtained in states where most of the array works in phase, as is the case with state "2".

Array properties

Several important properties of arrays of Fig. 3 can be derived from equations (5-10):

1) In the absence of external magnetic field:

- the UD array will be in phase for any DC bias; the in-phase state is a natural one for this array. Maximum power will be radiated at every operating frequency (Fig. 5.b).

- LR and CB arrays are symmetrical around the middle of the array; $m_{N-j} = -m_j$, which means that the junctions j and N-j are always in phase.

2) The LR array is equivalent to the LL array with equivalent external magnetic field $\varphi_{ex}' = \varphi_{ex} - \frac{N}{2} a$.

3) The larger the inductance parameter λ, the more in-phase states will be found in the given current bias span (eq. 8), and corresponding DC voltage and operating frequencies span. Similarly, the larger the array (N), the more identifiable "other" states will be found in the dV/dI-I curve (Fig. 5.a).

Magnetically steerable array

When an array is biased in the in-phase state ($i_{DC} = i_k$) the normalized relative time shift between every two neighboring junctions is the same and proportional to the external DC magnetic field:

$$\theta_j = \theta = \varphi_{ex} \bmod 1 , \qquad \forall j \tag{11}$$

This situation is shown in Figure 7. In Fig. 7.a the LL array is biased at the in-phase state (point "4", Fig. 5.a) with no external magnetic field. When an external magnetic field equal to a quarter of the flux quantum is applied, the time shift between the voltages of every two neighbors is equal to a quarter of period.

The time shift θT translates into the linear phase shift in the frequency domain $2\pi\theta$. Assuming that every junction drives one antenna, the quasioptical Josephson array becomes a phased array [9]. The angular position α_0 of the main beam in the H-plane far-field radiation pattern of the linear Josephson phased array becomes

$$\cos(\alpha_0) = -\frac{2\pi\theta}{\frac{2\pi}{\lambda_0} d_X} = -\frac{\theta}{d_X}\lambda_0 \qquad (12)$$

where d_X is the spacing between the antennas and λ_0 is the free space wavelength . The broadside radiation corresponds to $\alpha_0 = 90°$ ($\theta = 0$). Equations (11,12) suggest that by changing the externally applied DC magnetic field φ_{ex} it is possible to steer the Josephson array radiation pattern in the H-plane. As stated earlier, for the LL, LR and CB biased array, this is only true if the array is biased in the in-phase state. Since the UD array is always in the in-phase state, it can be steered using DC magnetic field at any bias.

Limitations

The expressions (9,10) derived for the "other" states will hold only in certain range of array parameters and bias conditions. We have derived expressions (5) for the in-phase states starting from (1) and assuming that all currents i_j are equal These expressions always hold for the in-phase states. The same expressions (5) are found for "other" states if we solve (1) with an assumption that DC currents $\langle i_j \rangle$ are approximately the same. The only part of the DC junction current that is different at every junction, due to DC self-field effects, is the supercurrent $\langle \sin(\phi_j) \rangle$. This part will be negligible if either the biasing current per junction is $\frac{i_{DC}}{N} >> 1$ or if there is non-vanishing capacitance ($\beta > 1$).

In our account of DC self-field effects we assumed the noiseless environment and the identical junctions. Therefore, the stability of in-phase and "other" states to noise and variations in junction and array parameters remains to be further investigated.

Strongly coupled arrays ($\lambda < 1$)

When the inductance parameter λ is small, it is evident from eq. (8) that the first in-phase state appears for very large DC biasing current, which translates into large DC voltage and operating frequency much above the critical frequency $\omega_c = (2e,\hbar)\, I_c\, R$. Depending on the capacitance parameter β and shunt resistance R, the operating frequency range is at best of the order of several ω_c. Therefore, the arrays with small inductances are operated in "other" states throughout the operating range. According to eq. (5), these states should be characterized with small time shifts between the junction phases/voltages. This is obvious, because in the limit of λ -> 0 the whole array operates as a single junction.

Figure 8.a presents simulations for 4 junction LL biased array with small inductance (λ = 0.628). The normalized harmonic radiated power is shown in the wide range of bias currents. The bias points a=0.25 and a=0.5 with no radiated first harmonic power correspond to the states where half of the junctions are in-phase and the other half out-of-phase, according to (5.a). As seen from the Figure 8.b, the maximum first harmonic power is below that of the UD array, with all junctions in-phase. Figure 9 compares the first harmonic power of 4- and 5-junction array with same parameters. The 5-junction array shows additional minimums in radiated power corresponding to states a=0.125 k. These minimums occur whenever there is one or more loops of array occupied by odd number of half-flux-quantums.

It is clear that in order for the array with small inductance to approach the performance of the UD array in the wide operating range, the condition for the inductance parameter must be $\lambda << \frac{1}{N}$. More precisely, if the total time shift across the array is required to be less than a quarter of a period, the condition is:

$$\lambda \; i_{DCmax} \leq \frac{\pi}{N+1} \qquad (13)$$

where i_{DCmax} is the DC bias at the end of the operating range. So, if we wanted a 4-junction LL biased array to approximately match the performance of UD array in Fig. 8.b, the inductance parameter should have been $\lambda = \frac{\pi}{120}$ instead of $\frac{\pi}{5}$. Such small inductances are rather unrealistic, specially because the λ parameter is proportional to the critical current I_c (eq. 1) which should be as large as possible for large output power.

As a final illustration, Figure 10 shows the influence of the Josephson junction capacitance.

The capacitance does not influence the occurrence or existence of in-phase and "other" states. However, it has a severe impact on radiated power. Even at not very big capacitance ($\beta = 3$) the first harmonic power is decreased at least an order of magnitude and the operating range is reduced below 2 ω_c.compared to the case of very small or no capacitance.

Conclusion

We have discussed how the DC biasing circuit determines the operation of linear parallel quasioptical Josephson junction arrays. We have shown that the maximum radiated power from the array can be achieved only at certain operating points, corresponding to the in-phase states. We have found that other states can be described by time-shifted phases and voltages of individual junctions, where the time-shift is determined from the DC biasing conditions. We have shown how the array can be steered from when in the in-phase state by application of DC magnetic field perpendicular to the array.

When the inductance parameter λ is large, there will be numerous in-phase bias points in the desired operating range. However, the stability of these states to noise and variations in junction parameters needs to be further investigated. When the inductance is relatively small, the radiated power will continuously change across the wide operating range, with several points where almost no power is radiated.

If one dimensional quasioptical arrays are designed, the UD biased array is a definite choice, because it is in the in-phase state at every bias point. The operation of this array need to be further analyzed when junction parameters are not identical. The extension of our considerations to 2-D arrays is straightforward, as long as rows of junctions are separately biased.

Acknowledgment

This work is supported by the Air Force Office of Scientific Research grant AFOSR-90-0233.

References

1. Robertazzi, R.P. and R.A. Buhrman, *Josephson terahertz local oscillator*. IEEE Trans. Magn., 1989. **25**: p. 1384-1387.

2. Wan, K., A.K. Jain and J.E. Lukens, *Submillimeter wave generation using Josephson junction arrays*. Appl. Phys. Lett., 1989. **54**: p. 1805-1807.

3. Benz, S.P. and C.J. Burroughs, *Coherent emission from two-dimensional Josephson junction arrays*. Appl. Phys. Lett., 1991. **58**(19): p. 2162-2164.

4. Wengler, M.J., A. Pance, B. Liu and R.E. Miller, *Quasioptical Josephson Oscillator*. IEEE Trans. Magn., 1991. **27**(2): p. 2708-2711.

5. Van Duzer, T. and C.W. Turner, *Principles of Supeconductive Devices and Circuits*. 1981, New York: Elsevier.

6. Ben-Jacob, E. and Y. Imry, *Dynamics of the DC-SQUID*. J. Appl. Phys., 1981. **52**(11): p. 6806-6815.

7. Press, W.H., B.P. Flannery, S.A. Teukolsky and W.T. Vetterling, *Numerical Recipes in C: The Art of Scientific Computing*. 1988, Cambridge, Mass.: Cambridge University Press.

8. Clarke, J. and T.A. Fulton, *Origin of Low-Voltage Structure and Asymmetry in the I-V Characteristics of Multiply-Connected Superconducting Junctions*. J. Appl. Phys., 1969. **40**(11): p. 4470-4476.

9. Steinberg, B.D., *Principles of Aperture and Array System Design*. 1976, New York: John Wiley & Sons, Inc.

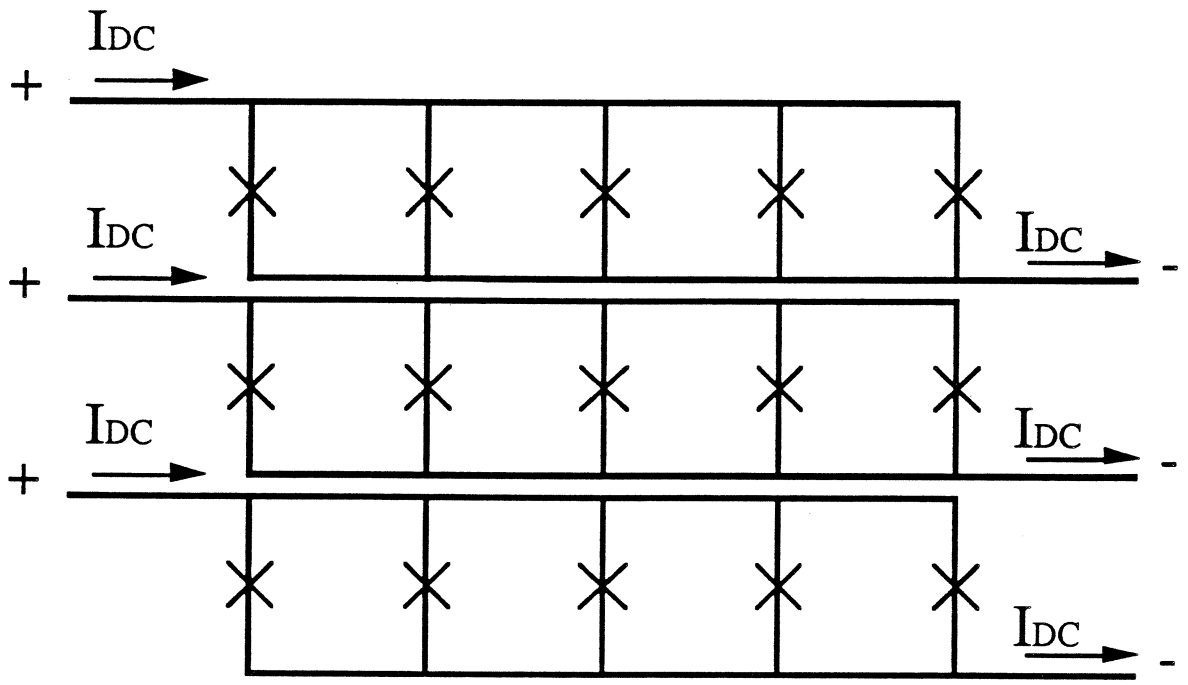

Figure 1. Separate row bias for parallel 2-D Josephson junction array.

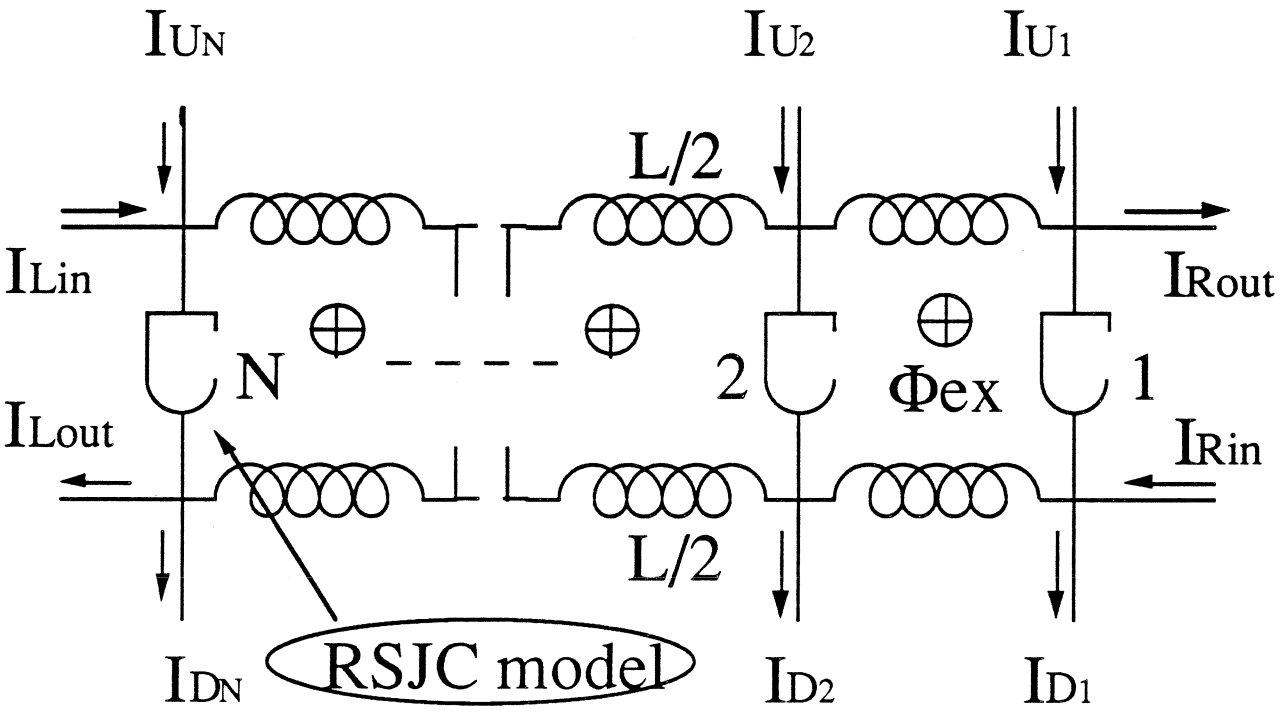

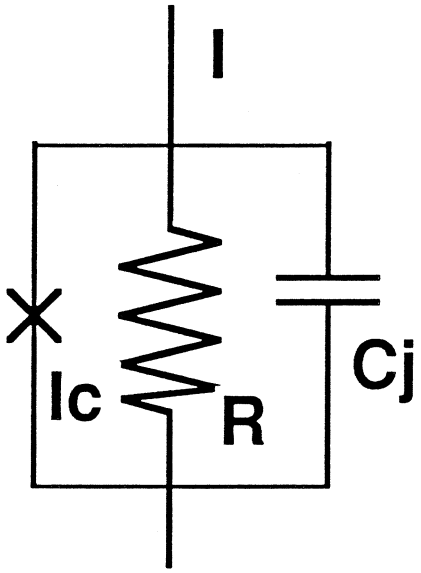

Figure 2. General biasing scheme for one-dimensional parallel Josephson junction array. The RSJC model used is shown below.

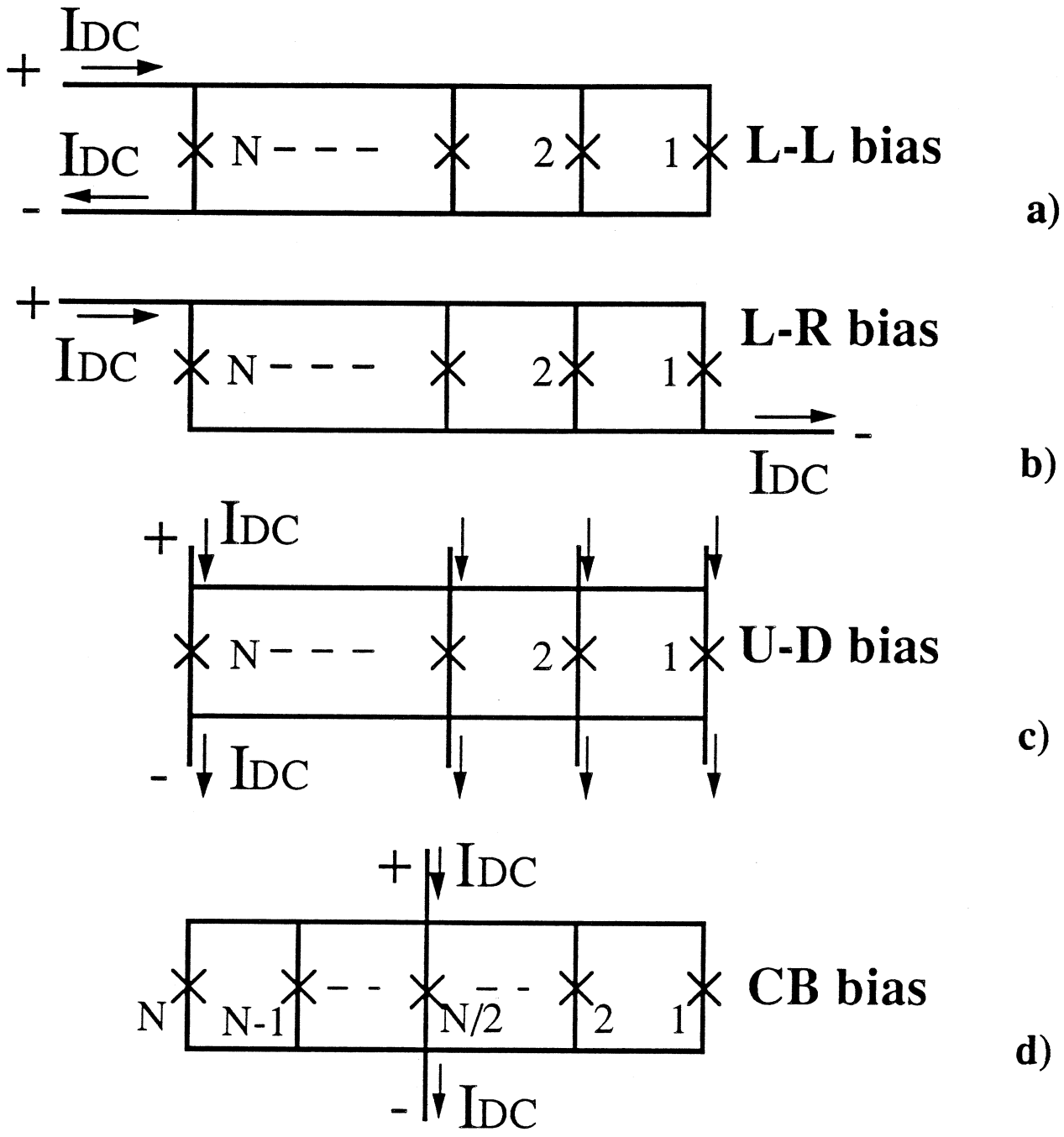

Figure 3. Four common biasing configurations of 1-D array.

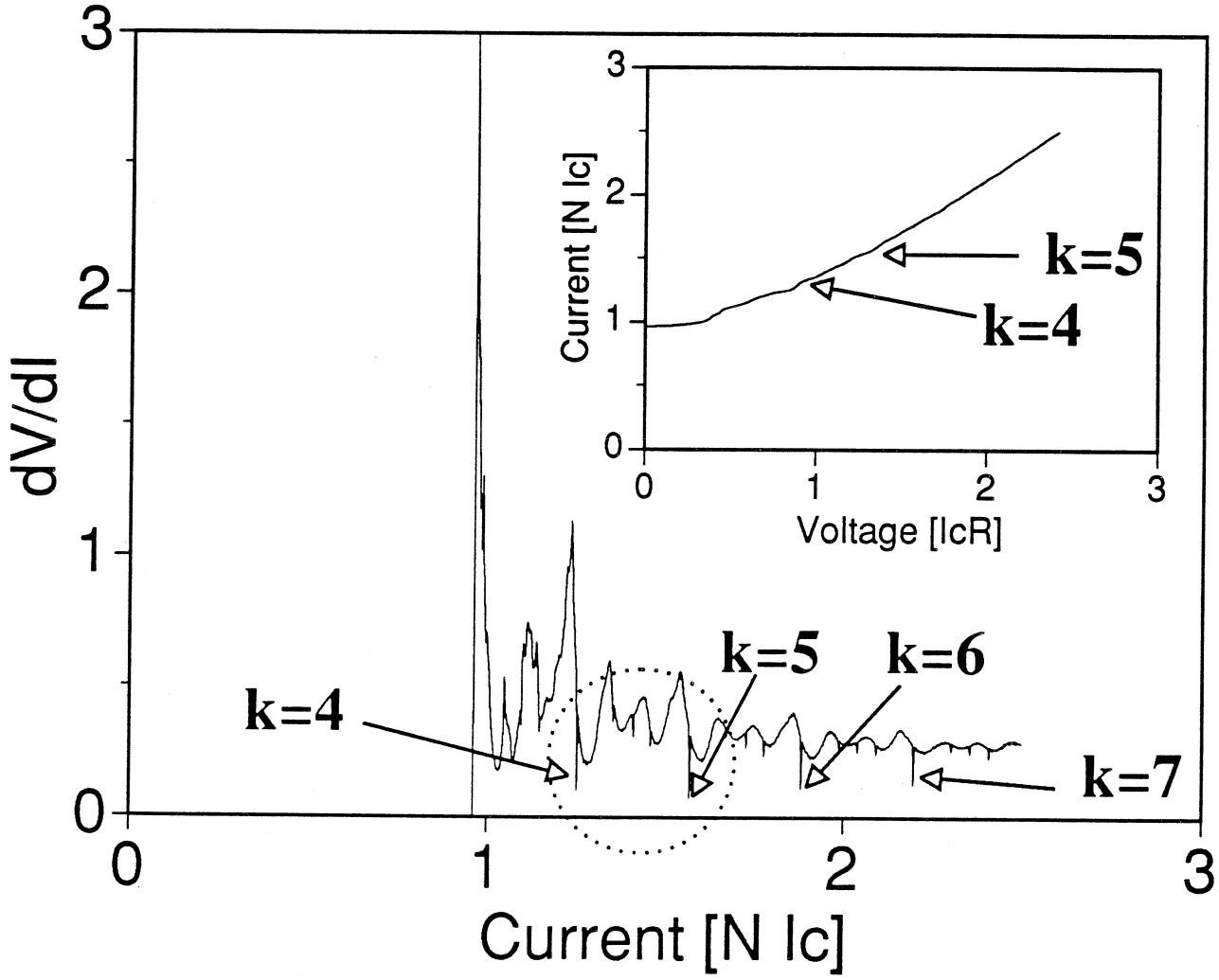

Figure 4. Dynamic resistance and I-V curve of 4 junction LL biased array with $\lambda = 20$ and $\beta = 0.5$. The in-phase states are seen as small steps in the I-V curve and sharp minimums in dV/dI-I curve , labeled k=4 to k=7. The area inside a circle is shown enlarged in Fig. 5.

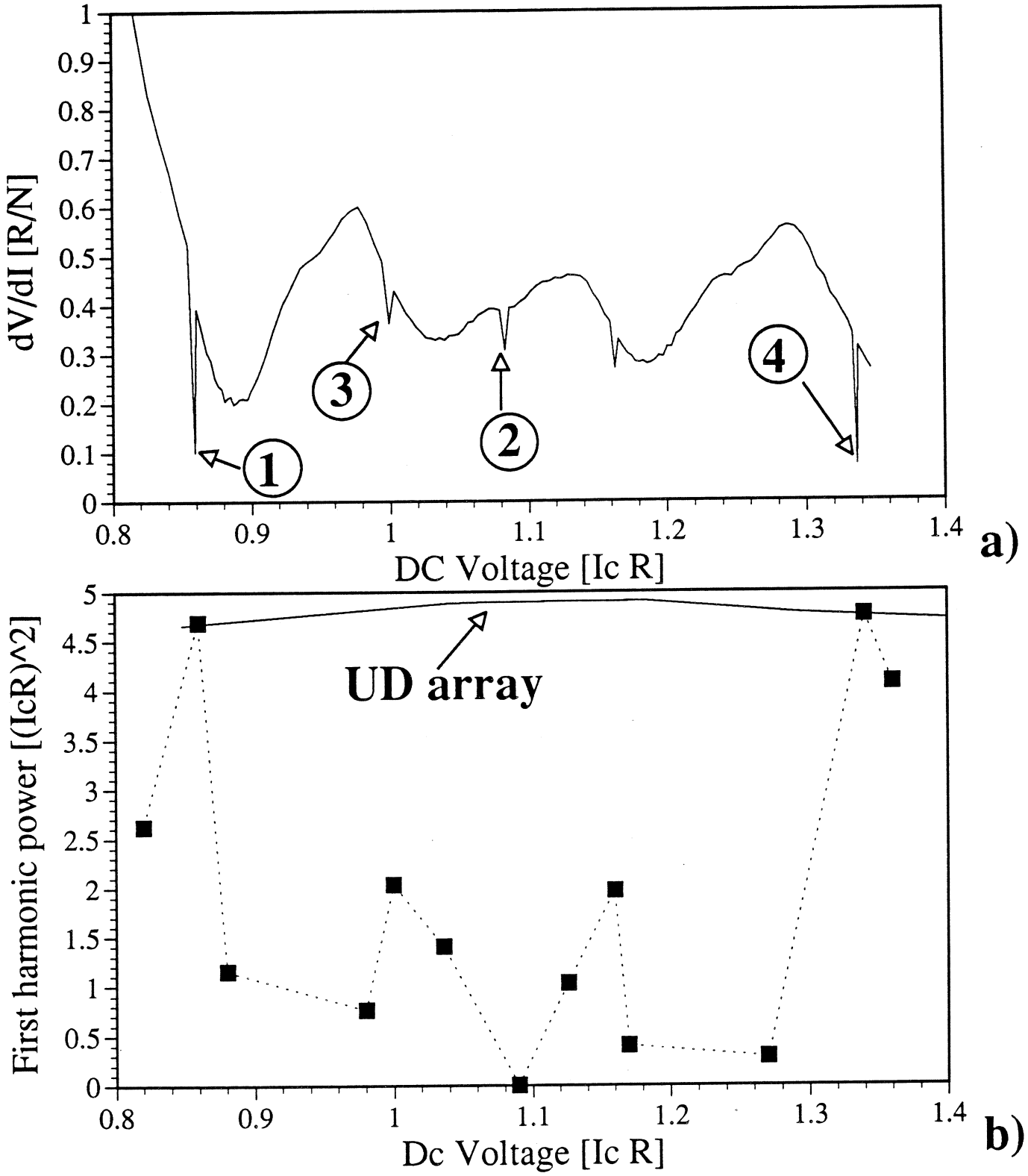

Figure 5. Four junction array, LL bias, $\lambda = 20$, $\beta = 0.5$. a) Enlarged portion of the dV/dI-I curve (Fig. 4) with in-phase states labeled "1" and "4" and two "other" states "2" and "3". The waveforms of individual junction voltages for these states are shown in Fig. 6 and 7. b) First harmonic power that correspond to states in a). The power is maximum in the in-phase states and equal to that of the equivalent UD array.

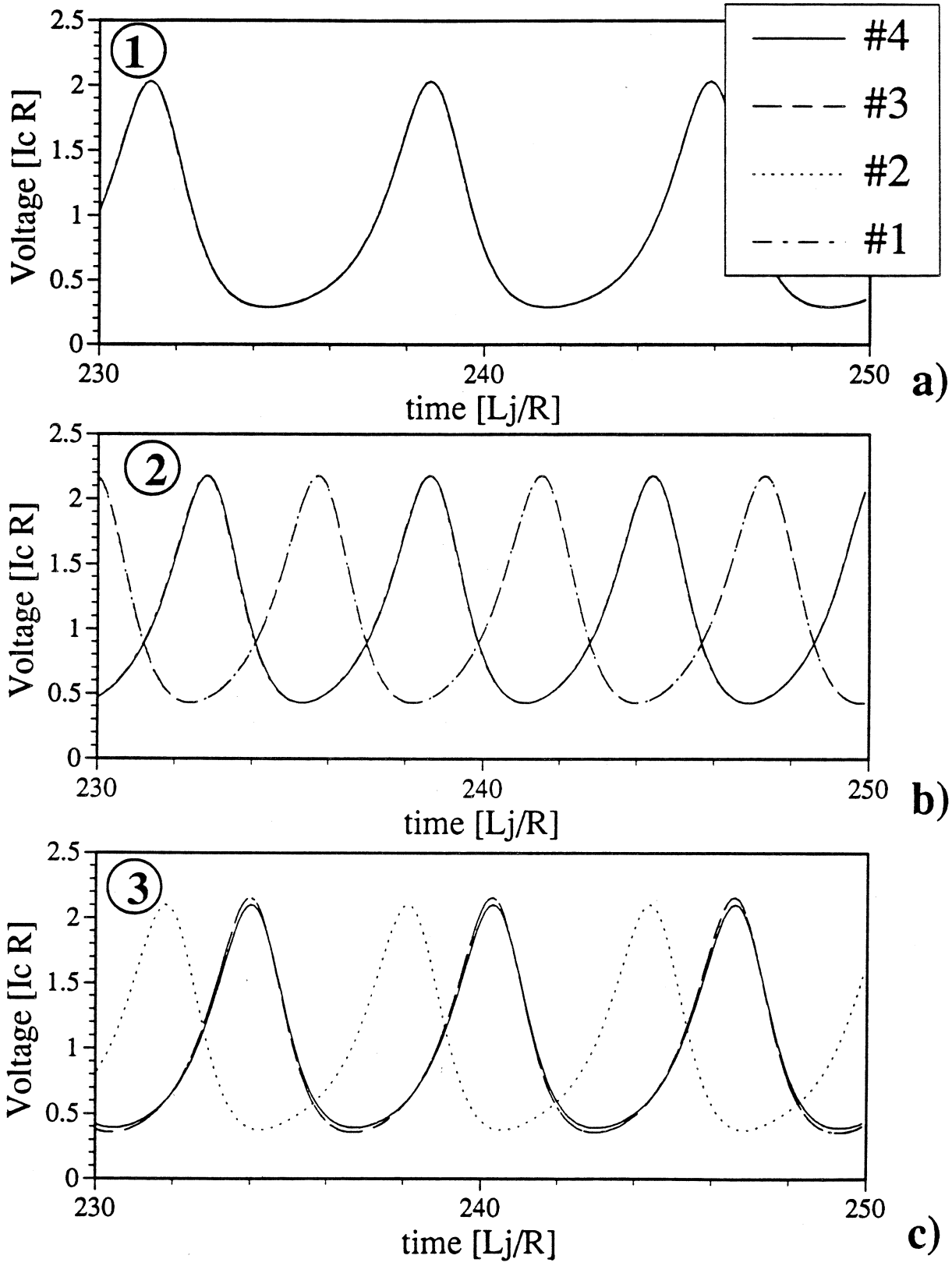

Figure 6. The waveforms of individual junction voltages for the states of Fig. 5. a) In-phase state. b) Junctions 1 &4 in phase, junctions 2 & 3 in phase , but out of phase with (1&4). No power radiated. c) Junctions 1,3 & 4 in phase, junction 2 "leads" a third of a period. Half the maximum power is radiated.

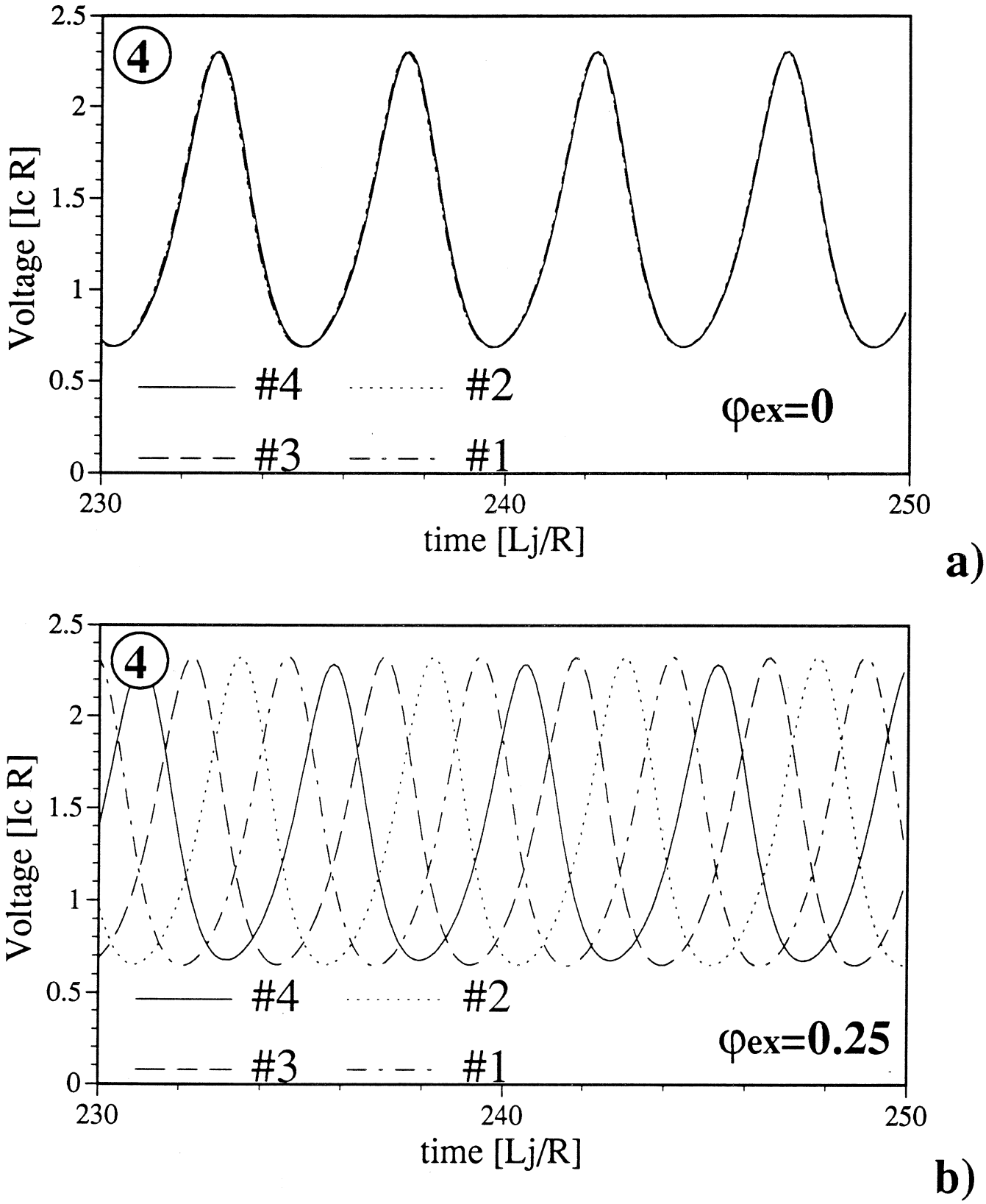

Figure 7. The waveforms of individual junction voltages for the in-phase state labeled "4" in Fig. 5. a) No DC magnetic field supplied. b) Quarter of the flux quantum in every loop supplied by the external magnetic field. Voltage waveforms uniformly shifted by quarter of a period. The main beam of the radiation is steered from the broadside direction.

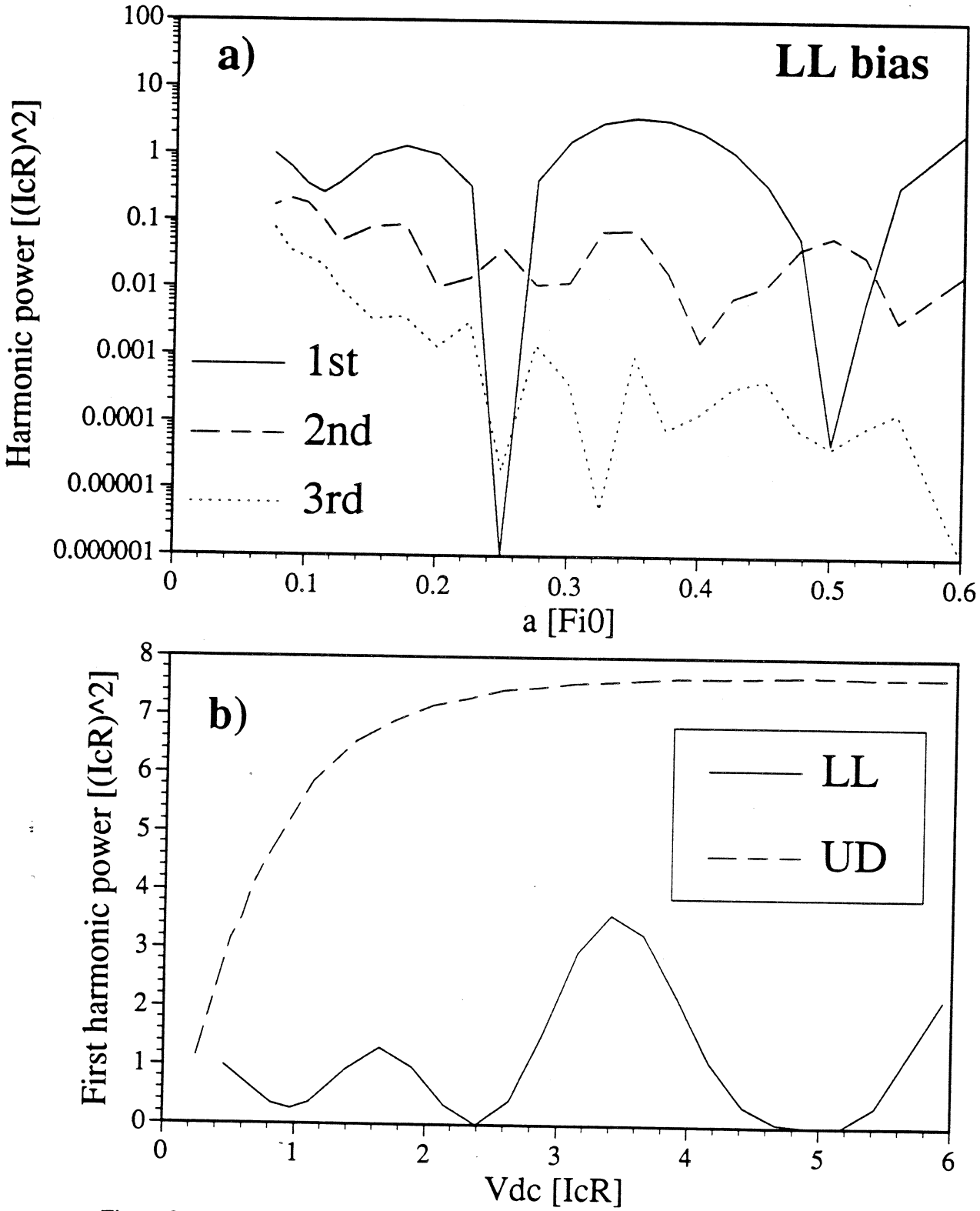

Figure 8. a) Harmonic power radiated by the 4-junction LL-biased array with $\lambda = \pi/5$ and $\beta = 0.03$. Minimums correspond to odd number of half-flux-quantums in some of the loops. b) Comparison between the LL and UD array with same parameters. Varying amount of power is radiated in the very broad operating range, but never a maximum possible power, as in the case of UD array.

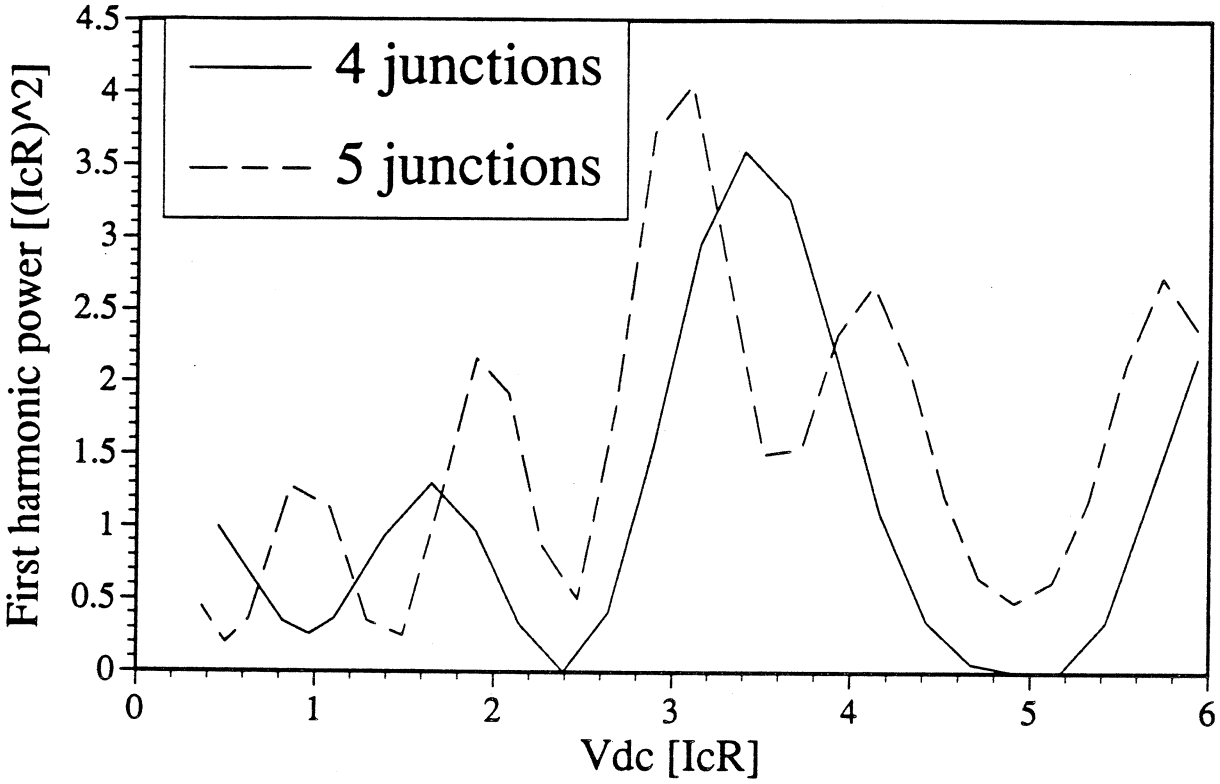

Figure 9. Comparison between the 4-junction and 5-junction small inductance arrays; $\lambda = \pi/5$, $\beta = 0.03$. As the number of junctions increase, more maximums and minimums appear throughout the operating range.

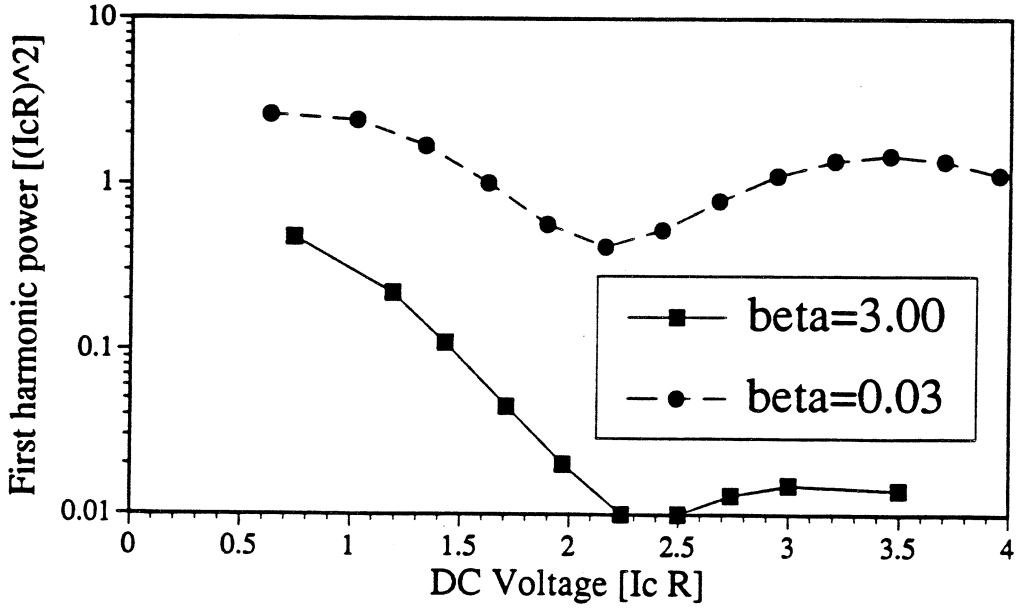

Figure 10. Four junction LL biased array, $\lambda = \pi/10$: Influence of the Josephson junction capacitance on power output. As the capacitance is increased, the maximum power and the operating range rapidly decreases.